On the stability of symplectic and energy-momentum algorithms for non-linear Hamiltonian systems with symmetry [☆]

O. Gonzalez[*,1], J.C. Simo

Division of Applied Mechanics, Department of Mechanical Engineering, Stanford University, Stanford, CA 94305, USA

Abstract

This paper presents a detailed comparison of two implicit time integration schemes for a simple non-linear Hamiltonian system with symmetry: the motion of a particle in a central force field. The goal is to establish analytical and numerical results pertaining to the stability properties of the implicit mid-point rule (the proto-typical implicit symplectic method) and a particular energy-momentum conserving scheme, and to compare the two schemes with respect to accuracy. While all results presented herein are within the context of a simple model problem, the problem was constructed so as to exhibit key features typical of more complex systems with symmetry such as those arising in non-linear solid mechanics; namely, the presence of large (and relatively slow) overall motions together with high-frequency internal motions.

Dedicated to the memory of Juan Carlos Simo

1. Introduction and motivation

In this paper we present a detailed comparison of two implicit time-integration schemes for a simple non-linear Hamiltonian system with symmetry: the motion of a particle in a central force field. The model problem is constructed so as to exhibit key features typical of more complex systems with symmetry such as those arising in non-linear solid mechanics; namely, the presence of large (and relatively slow) overall motions together with high-frequency internal motions. The two schemes considered are representative of two basic classes of implicit algorithms which are seemingly ideal for Hamiltonian systems: the so-called symplectic integrators and the conserving (or energy-momentum) algorithms.

First introduced in the work of DeVogelare [1] symplectic integrators are integration algorithms which preserve exactly the symplectic character of a Hamiltonian flow. Within the class of implicit schemes the classical example is the mid-point rule whose symplectic character was first noted in [2]; in particular, the entire Gauss family of implicit Runge–Kutta methods are symplectic as noted independently by Lasagni [3] and Sanz-Serna [4]. While symplectic integrators are geometrically appealing and have been shown to produce sharp phase portraits in long-term simulations, see e.g. [5–7], there is numerical evidence which shows that in general these algorithms can experience stability problems for stiff systems with symmetry (for examples see [8–11]).

As an alternative to (implicit) symplectic integrators we have the exact energy-momentum conserving algorithms which by design preserve the constants of motion (for specific examples see [8–16, 23]). This class of algorithms can be put within a general framework of discrete Hamiltonian systems with symmetry and can be shown to possess various notions of stability analogous to those of the underlying problem (see [17]).

The goal of this paper is to provide, within the simplest possible context, analytical results pertaining to the stability properties of the implicit mid-point rule (the prototypical implicit symplectic method) and a particular energy-momentum conserving scheme. For both algorithms we will examine notions of stability which are independent of integrability and dimension; in particular, general dynamic stability and relative Lyapunov stability of relative equilibria.

For the conserving scheme we will consider we can use general results on discrete Hamiltonian systems with symmetry to show that the scheme inherits the above notions of stability from the underlying model problem. However, since these results apply only to conserving schemes, we cannot use them directly to say anything about the mid-point rule. Hence, we introduce weaker notions of stability which can be 'easily' applied to both algorithms directly. For example, rather than analyze the relative Lyapunov stability of relative equilibria we introduce the notion of relative linear stability. This weaker notion can be applied in the same fashion to both the symplectic mid-point rule and the conserving scheme and hence will allow us to analytically compare stability properties of both schemes. (Note that from general results on discrete Hamiltonian systems with symmetry we know a priori that the conserving scheme inherits relative equilibria from the underlying system. At the moment we do not know if this is so for the symplectic mid-point rule.) We then verify the stability analysis numerically and end with a numerical comparison of accuracy.

2. The model problem

Consider a single particle of mass $m > 0$ in $\mathbb{R}^3$ moving about a fixed center of force which will be taken as the origin of an inertial coordinate system and denote the position of the particle by $q \in \mathbb{R}^3$. We restrict ourselves to conservative central forces with potential $U : \mathbb{R}^3 \to \mathbb{R}$ where the potential is by necessity a function of the radial distance $|q|$ only, i.e. $U(q) = V(|q|)$ where $V : \mathbb{R}_+ \to \mathbb{R}$. (Here, $|\cdot|$ denotes the standard Euclidean norm on $\mathbb{R}^3$.) For any motion of the system $t \mapsto q(t) \in \mathbb{R}^3$ Newton's second law requires

$$m\ddot{q} = -\nabla U(q) = -\frac{V'(|q|)}{|q|}\, q \; . \tag{2.1}$$

REMARKS 2.1.
(1) For celestial mechanics applications an identical equation governs the dynamics of the classical two-body problem after reduction to the center of mass [18]. In this case m is interpreted as the reduced mass and q as the relative position vector defined for the two-body system as

$$\begin{aligned} m &= m_1 m_2 / (m_1 + m_2) \; , \\ q &= q_2 - q_1 \; . \end{aligned} \tag{2.2}$$

The system in (2.1) reduces to the well-known Kepler problem when the potential is of the form $V(|q|) = -k/|q|$ for some real number $k > 0$.
(2) To model situations arising in solid mechanics we consider the potential V to be that of a stiff (non-linear) spring with free length λ_0. That is, $V'(\lambda_0) = 0$ and V'' large and positive in a neighborhood of λ_0. For example, $V(\lambda) = \frac{1}{2}k(\lambda^2 - \lambda_0^2)^2$ for some constant $k > 0$.

3. Hamiltonian formulation and conservation laws

Define the momenta of the particle by the expression $p = m\dot{q}$ and consider rewriting (2.1) in first-order form on a phase space $P = \mathbb{R}^3 \times \mathbb{R}^3 \cong \mathbb{R}^6$ as

$$\dot{q} = m^{-1}p \,,$$

$$\dot{p} = -\frac{V'(|q|)}{|q|}\, q \,. \tag{3.1}$$

Let $z = (q^T, p^T)^T \in P$. Then, (3.1) defines a Hamiltonian system on P as follows (see [19] for an explanation of the terminology and notation used below). Define the Hamiltonian function $H: P \to \mathbb{R}$ by

$$H(z) = \frac{1}{2m}\, |p|^2 + V(|q|) \,, \tag{3.2}$$

and consider the standard two-form $\Omega: TP \times TP \to \mathbb{R}$ given by the expression

$$\Omega_{(z)}(\delta z_1, \delta z_2) = \delta z_1^T \mathbf{J}\, \delta z_2 \quad \text{where} \quad \mathbf{J} = \begin{bmatrix} 0 & 1 \\ -1 & 0 \end{bmatrix}, \tag{3.3}$$

for all $z \in P$ and $\delta z_\alpha \in T_z P \cong \mathbb{R}^6$ ($\alpha = 1, 2$). In view of (3.2) and (3.3) we conclude that Eqs. (3.1) for the motion $t \mapsto z(t) \in P$ can be written in Hamiltonian form as

$$\dot{z} = \mathbf{J}\nabla H(z) \,. \tag{3.4}$$

Consider now the (symplectic) action of the rotation group $G = \mathrm{SO}(3)$ on P defined by

$$\Phi(\Lambda, (q, p)) = (\Lambda q, \Lambda^{-T} p)$$
$$= (\Lambda q, \Lambda p) \,, \tag{3.5}$$

where $\Lambda \in G$. Since H is invariant under Φ we have a Hamiltonian system with symmetry. Furthermore, the action Φ possesses a momentum map $J: P \to T_e^* G \cong \mathbb{R}^3$ given by $J(q, p) = q \times p$ which is called the angular momentum for the system. Given this structure the dynamics described by Hamilton's equations (3.1) or (3.4) give rise to a flow on the phase space P with the following properties.

(1) *Conservation of energy.* The Hamiltonian (i.e. the total energy of the system) is conserved along solutions $t \mapsto z(t) \in P$ of Hamilton's equations, i.e.

$$\frac{\mathrm{d}}{\mathrm{d}t}\, H(z(t)) = 0 \,. \tag{3.6}$$

(2) *Conservation of total angular momentum.* The angular momentum map $J: P \to \mathbb{R}^3$ defined by $J(z) = q \times p$ is conserved along solutions $t \mapsto z(t) \in P$, i.e.

$$\frac{\mathrm{d}}{\mathrm{d}t}\, J(z(t)) = \mathbf{0} \,. \tag{3.7}$$

(3) *Symplectic character of Hamiltonian flow.* For any $z_0 \in P$ the local flow F generated by (3.4) is a symplectic map on (P, Ω) for each t for which it is defined. In particular, for each $z_0 \in P$ there is a neighborhood U of z_0 and an interval I in $\mathbb{R}$ containing the origin and a map $F: U \times I \to P$ which is locally a flow for the Hamiltonian system of ordinary differential equations. That is, for any $z \in U$ the curve defined by $\varphi(t) = F(z, t) = F_t(z)$ is a solution with initial condition $\varphi(0) = z$. For each $t \in I$ the mapping $F_t: U \to P$ is symplectic in the sense that

$$D_z F_t^T\, \mathbf{J}\, D_z F_t = \mathbf{J} \,, \quad \forall z \in U \,, \tag{3.8}$$

where $D_z F_t$ is the derivative of F_t at $z \in U$ (for more details see [19]).

REMARK 3.1. Integrators for which the symplectic condition (3.8) is satisfied by the algorithmic flow $\mathbb{F}_{\Delta t}$ are called symplectic integrators. Within the class of implicit Runge–Kutta methods, the so-called Gauss family satisfy this condition (see e.g. [3, 4]). The best known example is the implicit mid-point rule [2].

4. Notions of stability

For Hamiltonian systems with symmetry we consider two basic notions of stability which are independent of integrability and dimension: general dynamic stability and relative Lyapunov stability of relative equilibria. The first deals with boundedness of solutions uniformly in time and the second with the behavior of solutions beginning in a neighborhood of a relative equilibrium solution (i.e. an invariant set).

4.1. General dynamic stability

Recall that a solution $(q(t), p(t))$ of (3.4) with initial condition (q_0, p_0) is said to be dynamically stable if there is a constant $K > 0$ such that $\|(q(t), p(t))\| \leq K$ for all $t \geq 0$. (Here, $\| \cdot \|$ denotes the standard Euclidean norm on P.) We now investigate the dynamic stability of solutions to (3.4) for two classes of potentials:

(1) *Non-linear spring potential*. The potential $V : \mathbb{R}_+ \to \mathbb{R}$ is of the form $V(\lambda) = \frac{1}{2} k (\lambda^2 - \lambda_0^2)^2$ for some constants $k > 0$ and $\lambda_0 > 0$. Note that $V(\lambda) \geq 0$ for all $\lambda \in \mathbb{R}_+$ and $V(\lambda) \to \infty$ as $\lambda \to \infty$. To assess dynamic stability note that a solution $(q(t), p(t))$, while it exists, remains in a level set $H^{-1}(c) \subset P$ where $c \geq 0$ is determined by the initial condition, i.e. $H(q_0, p_0) = c$. Now, while a solution exists we have

$$H(q(t), p(t)) = \frac{1}{2} m^{-1} |p(t)|^2 + V(|q(t)|) = c . \tag{4.1}$$

So

$$V(|q(t)|) \leq c \quad \text{and} \quad |p(t)|^2 \leq 2mc . \tag{4.2}$$

Hence, while they exist, solutions are bounded. Since we are dealing with smooth Hamiltonians only this implies that solutions are defined for all $t \geq 0$. For any solution we can thus find a constant $K > 0$ such that $\|(q(t), p(t))\| \leq K$ for all $t \geq 0$.

(2) *Kepler potential*. The potential $V : \mathbb{R}_+ \to \mathbb{R}$ is of the form $V(\lambda) = -k/\lambda$ for some constant $k > 0$. Note that $V(\lambda) \leq 0$ for all $\lambda \in \mathbb{R}_+$, $V(\lambda) \to 0$ as $\lambda \to \infty$, and $V(\lambda) \to -\infty$ as $\lambda \to 0$. To assess dynamic stability we note that a solution $(q(t), p(t))$, while it exists, remains in a level set $H^{-1}(c) \subset P$ where $c \in \mathbb{R}$ is determined by the initial condition, i.e. $H(q_0, p_0) = c$. In this case, however, we cannot show that solutions are bounded using only level sets of the Hamiltonian. We now have to use some of the symmetry properties, namely, the fact that the momentum map J is conserved along solutions. Suppose the initial condition is such that $J(q_0, p_0) = \mu$ which implies $(q(t), p(t)) \in H^{-1}(c) \cap J^{-1}(\mu)$. Given the notion of a reduced system (to be introduced in the next section) we have that the following quantity

$$\tilde{H}(|q|, \pi) = \pi^2/2m + |\mu|^2/2m|q|^2 + V(|q|) \tag{4.3}$$

is conserved along solutions. In particular, $\tilde{H}$ is the reduced Hamiltonian which we will derive shortly and $\pi \in \mathbb{R}$ is the reduced momentum variable defined such that $|p|^2 = \pi^2 + |\mu|^2/|q|^2$. Now, while a solution exists we have

$$\pi^2/2m + |\mu|^2/2m|q|^2 - k/|q| = c . \tag{4.4}$$

Assuming $c = -|c| < 0$ we get $-k/|q| \leq -|c|$ which implies

$$|q(t)| \leq k/|c| . \tag{4.5}$$

Also from (4.4) and the assumption $c < 0$ we have $|\mu|^2/2m|q|^2 - k/|q| \leq 0$ which implies

$$|q(t)| \geq |\mu|^2/2mk . \tag{4.6}$$

Hence, $H(q_0, p_0) = c < 0$ implies that $|q(t)|$ is bounded. Similarly for $|\pi(t)|$ and hence $|p(t)|$. Thus, for any solution with initial condition satisfying $H(q_0, p_0) = c < 0$ we can find a constant $K > 0$ such that $\|(q(t), p(t))\| \leq K$ for all $t \geq 0$.

Clearly, any energy-momentum conserving approximation scheme (which conserves the reduced

Hamiltonian) inherits this notion of stability from the underlying system. It is not clear, however, that similar infinite-time results (independent of the time step) can be deduced for the mid-point rule on a six-dimensional phase space.

4.2. Relative equilibria, reduction and relative stability

Given the Hamiltonian system with symmetry (P, Ω, G, H) with momentum map $J: P \rightarrow T_e^* G$ recall that a relative equilibrium with momentum μ is a point $(q_e, p_e) \in J^{-1}(\mu) \subset P$ with the property that the solution through it satisfies

$$
\begin{aligned}
(q(t), p(t)) &= \Phi(\exp[t\hat{\xi}], (q_e, p_e)) \\
&= (\exp[t\hat{\xi}]q_e, \exp[t\hat{\xi}]p_e) ,
\end{aligned}
\tag{4.7}
$$

for some $\hat{\xi} \in T_e G = \mathrm{so}(3)$ where $\exp[\cdot]$ is the matrix exponential and so(3) denotes the set of real 3×3 skew-symmetric matrices. In particular, a relative equilibrium point $(q_e, p_e) \in J^{-1}(\mu) \subset P$ may be characterized as a critical point of the Hamiltonian H *restricted* to the level set $J^{-1}(\mu)$ (see e.g. [20–22]). Regarding Lyapunov stability for the relative equilibrium point, the most that we can say is with respect to the set

$$
[(q_e, p_e)] = \{(q, p) \in P \,|\, (q, p) = \Phi(\Lambda, (q_e, p_e)), \Lambda \in G_\mu\} \subset J^{-1}(\mu) ,
\tag{4.8}
$$

where G_μ is the subgroup of G under which the level set $J^{-1}(\mu)$ is invariant (i.e. $\Phi_g: P \rightarrow P$ leaves this set invariant for all $g \in G_\mu$). In particular, Lyapunov stability for the set $[(q_e, p_e)]$ *within the momentum level set*, which is defined as *relative* Lyapunov stability for the point (q_e, p_e), may be defined using the notions of reduction and reduced systems. Briefly, given a regular value μ for J we can restrict the original Hamiltonian system to the level set $J^{-1}(\mu)$ and then 'factor out' those group motions that leave this level set invariant. The result is a Hamiltonian system $(\tilde{P}, \tilde{\Omega}, \tilde{H})$ which is called the reduced system. By design, the set $[(q_e, p_e)]$ in $J^{-1}(\mu) \subset P$ corresponds to a critical point $\tilde{z}_e \in \tilde{P} = J^{-1}(\mu)/G_\mu$ of the reduced system and we say that the set $[(q_e, p_e)]$ is stable within $J^{-1}(\mu)$ if the critical point of the reduced system is stable. That is, a relative equilibrium point $(q_e, p_e) \in P$ is relatively Lyapunov stable if the associated fixed point for the reduced system is Lyapunov stable.

By general results for discrete Hamiltonian systems with symmetry the constructions outlined above carry over to a large class of conserving approximation schemes such as those considered herein. Hence, for the conserving scheme we consider, if the underlying system possesses a relatively stable relative equilibrium point so does the algorithm. We cannot, however, use the above constructions to conclude the same for the mid-point rule. In order to 'compare' stability properties of both approximation schemes we thus carry out the reduction process in detail for the underlying problem and introduce a weaker notion of relative stability applicable to both algorithms. Our goal is to introduce a framework in which to analytically compare the stability properties of the symplectic mid-point and conserving algorithms, at least within the context of relative equilibria.

4.2.1. Reduction

In this section we review the notion of reduction for the model problem. The ideas presented are well-known (see e.g. [18, Chapter 3]) and are outlined below merely to motivate the procedure for the algorithmic setting.

Let $\{e_1, e_2, e_3\}$ be a fixed orthonormal basis in $\mathbb{R}^3$ and let $J(z_0) = \mu \neq 0$. (The case $\mu = 0$ is degenerate and corresponds to motion along a straight line through the origin.) Since J is constant during any motion and by construction $q \cdot J = 0$ and $p \cdot J = 0$, we conclude that q and p remain in a plane $\Gamma \subset \mathbb{R}^3$ where $\Gamma = \{x \in \mathbb{R}^3: x \cdot \mu = 0\}$.

Assume for simplicity that μ is parallel to e_3 and introduce plane polar coordinates $(\lambda, \vartheta) \in \mathbb{R}_+ \times S^1$ in Γ. In addition, let $\{e, e^\perp, e_3\}$ be a moving orthonormal frame defined by the expressions

$$e = q/|q| \, ,$$
$$e_3 = \mu/\mu \, ,$$
$$e^\perp = e_3 \times e \, ,$$
(4.9)

and let ϑ be defined such that the orientation of e with respect to the fixed frame is

$$e = \cos(\vartheta)e_1 + \sin(\vartheta)e_2 \, .$$
(4.10)

From (4.10) and (4.9) we see that $\{e, e^\perp\}$ span Γ and have time derivatives given by

$$\dot{e} = \vartheta e^\perp \, ,$$
$$\dot{e}^\perp = -\vartheta e \, .$$
(4.11)

To obtain the reduced equations of motion we express $q, p \in \Gamma$ in the moving frame as

$$q = \lambda e \, ,$$
$$p = \pi e + \eta e^\perp \, ,$$
(4.12)

and note immediately that the condition $\mu = q \times p$ implies $\eta = \mu/\lambda$. Substituting (4.12) into Hamilton's equations (3.1) gives the following evolution equations for the reduced variables:

$$\dot{\vartheta} = \mu/m\lambda^2 \, , \qquad \vartheta \in S^1 \, ,$$
$$\dot{\lambda} = \pi/m \, , \qquad \lambda \in \mathbb{R}_+ \, ,$$
$$\dot{\pi} = -V'(\lambda) + \mu^2/m\lambda^3 \, , \quad \pi \in \mathbb{R} \, .$$
(4.13)

In the present case the reduced equations have a particularly simple form. Note that the evolutions for λ and π are independent of ϑ. Once λ has been determined as a function of time, Eq. (4.13)$_1$ may be integrated to determine ϑ. (In this case ϑ is said to be a cyclic or ignorable coordinate.) Hence, the reduced dynamics are completely characterized by the evolution of λ and π. We now show that the reduced equations (4.13)$_{2,3}$ are Hamiltonian with phase space $\tilde{P} = \{(\lambda, \pi)^\mathrm{T} \in \mathbb{R}^2 \colon \lambda \in \mathbb{R}_+\}$.

Let $\tilde{z} = (\lambda, \pi)^\mathrm{T} \in \tilde{P}$. Then, (4.13)$_{2,3}$ define a Hamiltonian system on $\tilde{P}$ as follows. Define the reduced Hamiltonian function $\tilde{H} \colon \tilde{P} \to \mathbb{R}$ by

$$\tilde{H}(\tilde{z}) = \frac{1}{2m} \pi^2 + V_\mu(\lambda) \, ,$$
(4.14)

where $V_\mu(\lambda) = V(\lambda) + \mu^2/2m\lambda^2$ and consider the standard two-form $\tilde{\Omega} \colon T\tilde{P} \times T\tilde{P} \to \mathbb{R}$ given by the expression

$$\tilde{\Omega}_{(\tilde{z})}(\delta\tilde{z}_1, \delta\tilde{z}_2) = \delta\tilde{z}_1^\mathrm{T} \tilde{\mathbf{J}} \, \delta\tilde{z}_2 \quad \text{where} \quad \tilde{\mathbf{J}} = \begin{bmatrix} 0 & 1 \\ -1 & 0 \end{bmatrix} .$$
(4.15)

In view of (4.14) and (4.15) we conclude that Eqs. (4.13)$_{2,3}$ for the motion $t \mapsto \tilde{z}(t) \in \tilde{P}$ can be written in Hamiltonian form as

$$\dot{\tilde{z}} = \tilde{\mathbf{J}} \nabla \tilde{H}(\tilde{z}) \, .$$
(4.16)

REMARKS 4.1.

(1) Note that the reduction followed from the conservation of total angular momentum; in particular, the conservation of energy played no role in the reduction process. This observation is crucial in the algorithmic setting.

(2) The potential V_μ in the reduced Hamiltonian is the sum of the original potential V and the potential of the centrifugal force. In the mechanics literature, V_μ is known as the amended potential and arises in the study of relative equilibria for Hamiltonian systems with symmetry.

(3) In this case the reduced equations are Hamiltonian relative to the standard two-form $\tilde{\Omega}$ on $\tilde{P} \subset \mathbb{R}^2$. In the general case, reduction yields equations which are Hamiltonian relative to a *non-standard* two-form.

(4) As required by the symplectic reduction theorem [22], the reduced flow in $\tilde{P}$ is a symplectic map

for each $t > 0$ relative to the two-form $\tilde{\Omega}: T\tilde{P} \times T\tilde{P} \to \mathbb{R}$. In particular, for each $t > 0$ the reduced flow is an area-preserving map of $\tilde{P}$ into itself.

4.2.2. Relative equilibria and relative linear stability
Consider a fixed point $\tilde{z}^* \in \tilde{P}$ of the reduced equations (4.16) which in components are

$$\dot{\lambda} = \pi/m \,, \qquad (4.17)$$
$$\dot{\pi} = -V'_\mu(\lambda) \,.$$

Clearly, the fixed point must be of the form $\tilde{z}^* = (\lambda^*, 0)^\mathrm{T}$ where λ^* is a stationary point of the amended potential V_μ. Inspection of Eqs. (4.11)–(4.13) shows that a fixed point of the reduced Hamiltonian flow on $\tilde{P}$ corresponds to a steady motion on the canonical phase space P. This steady solution is a relative equilibria for the system on P. In terms of the motion of the particle in $\mathbb{R}^3$, the relative equilibria corresponds to a steady circular orbit of the particle in the plane Γ with radius $|q| = \lambda^*$.

We now introduce the notion of relative linear stability for a relative equilibria. In particular, we will say that a relative equilibria is *relatively linearly stable* if the fixed point of the reduced equations in $\tilde{P}$ is linearly stable, which we define next.

Let $\tilde{F}_t: \tilde{P} \to \tilde{P}$ be the t-advance mapping for the solution of the reduced equations, i.e. $\tilde{z}_t = \tilde{F}_t(\tilde{z}_0)$, and note that by definition the fixed point $\tilde{z}^*$ satisfies $\tilde{z}^* = \tilde{F}_t(\tilde{z}^*)$ for all $t \geq 0$. We say that $\tilde{z}^*$ is *linearly stable* if infinitesimal disturbances $\delta\tilde{z} \in T_{\tilde{z}^*}P$ on $\tilde{z}^*$ do not grow in time. To examine the linear stability of $\tilde{z}^*$ we must consider the derivative $D_{\tilde{z}^*}\tilde{F}_t: T_{\tilde{z}^*}\tilde{P} \to T_{\tilde{z}^*}\tilde{P}$. First, note that as in the canonical case the mapping $\tilde{F}_t$ is symplectic on $\tilde{P}$ for each $t > 0$. Hence, the condition (3.8) implies

$$\det[D_{\tilde{z}}\tilde{F}_t] = 1 \,, \quad \forall\, t > 0 \,, \quad \forall\, \tilde{z} \in \tilde{P} \,, \qquad (4.18)$$

so that $\tilde{F}_t$ is an area-preserving map of $\tilde{P} \subset \mathbb{R}^2$ into itself. Now consider an infinitesimal disturbance $\delta\tilde{z}$ on the solution $\tilde{z}^*$. The infinitesimal disturbance satisfies the equation of variations

$$\delta\dot{\tilde{z}}_t = \tilde{J}\nabla^2\tilde{H}(\tilde{z}^*)\,\delta\tilde{z}_t \,, \qquad (4.19)$$

which may be solved as

$$\delta\tilde{z}_t = \exp[\tilde{J}\nabla^2\tilde{H}(\tilde{z}^*)t]\,\delta\tilde{z}_0 = A_t\,\delta\tilde{z}_0 \,. \qquad (4.20)$$

Hence, the evolution of the infinitesimal disturbance $\delta\tilde{z}$ is determined by the one-parameter group of transformations $A_t = D_{\tilde{z}^*}\tilde{F}_t: T_{\tilde{z}^*}\tilde{P} \to T_{\tilde{z}^*}\tilde{P}$. From (4.20) we see that infinitesimal perturbations of the fixed point $\tilde{z}^*$ remain infinitesimal if the mapping A_t is stable. In view of (4.18) stability of this mapping requires that the eigenvalues $\zeta_{1,2}(A_t)$ be simple on the unit circle in the complex plane. Since $A_t \in \mathbb{R}^{2\times2}$ we have

$$\zeta_{1,2}(A_t) = \frac{1}{2}\,\mathrm{tr}[A_t] \pm \sqrt{\frac{1}{4}\,\mathrm{tr}^2[A_t] - 1} \,, \qquad (4.21)$$

so that the eigenvalues are simple on the unit circle if

$$\left|\frac{1}{2}\,\mathrm{tr}[A_t]\right| < 1 \,. \qquad (4.22)$$

From the preceding results we conclude that the linear stability of the fixed point $\tilde{z}^* = (\lambda^*, 0)^\mathrm{T} \in \tilde{P}$ (and hence relative linear stability of the relative equilibria on P) is determined by the trace of the linearized t-advance mapping $A_t = D_{\tilde{z}^*}\tilde{F}_t$.

REMARK 4.2. In the present case, linear stability of the fixed point $\tilde{z}^*$ implies that λ^* is a local minimum of the amended potential, i.e. $V''_\mu(\lambda^*) > 0$. This follows from (4.20) where a simple calculation gives the eigenvalues of A_t as

$$\zeta_{1,2}(A_t) = \exp[\pm i\sqrt{V''_\mu(\lambda^*)/m}\;t] \,. \qquad (4.23)$$

It then follows that the condition for linear stability is equivalent to $V''_\mu(\lambda^*) > 0$ which implies non-linear stability of the fixed point (and hence the relative equilibria). This, however, does not hold for the general case. That is, linear stability does not generally imply non-linear (Lyapunov) stability. Throughout the remainder of our analysis we assume that the model problem has a stable relative equilibria in the sense that $V''_\mu(\lambda^*) > 0$.

5. Symplectic approximation: Implicit mid-point rule

In the following sections we consider the mid-point algorithm and address the question of relative linear stability for a relative equilibria of the *discrete* dynamics. Beginning with the mid-point rule formulated on the canonical phase space $P = \mathbb{R}^3 \times \mathbb{R}^3$ we will show that the discrete dynamics may be reduced to the phase space $\bar{P} \subset \mathbb{R}^2$. We then show that a fixed point exists for the reduced algorithmic equations and analyze the linear stability of this fixed point by way of the linearized algorithmic Δt-advance mapping. For purposes of comparison, we then formulate the mid-point rule directly on the reduced space $\bar{P}$ and perform a similar analysis.

5.1. Algorithmic approximation on original phase space

Let $[0, T]$ be the time interval of interest and consider the equations of motion on P given in (3.1) or (3.4) with initial data $z(0) = z_0$. Given a partition $\{t_n\}_{n=0}^N$ of $[0, T]$ such that $t_0 = 0$, $t_N = T$, and $t_{n+1} - t_n = \Delta t > 0$, the algorithmic problem is to compute z_{n+1} from given data $z_n \in P$ and generate a solution sequence $(z_n)_{n=0}^N$ where z_n stands for an algorithmic approximation to $z(t_n)$. The mid-point approximation to (3.4) is

$$z_{n+1} - z_n = \Delta t \, \mathbf{J}\nabla H(z_{n+1/2}) \,, \tag{5.1a}$$

where $(\cdot)_{n+1/2} = \frac{1}{2}[(\cdot)_n + (\cdot)_{n+1}]$. In view of (3.1) the explicit form of (5.1a) is

$$q_{n+1} - q_n = \Delta t \, m^{-1} p_{n+1/2} \,, \tag{5.1b}$$
$$p_{n+1} - p_n = -\Delta t \, \frac{V'(|q_{n+1/2}|)}{|q_{n+1/2}|} \, q_{n+1/2} \,.$$

REMARK 5.1. For the discrete dynamics defined by the mid-point algorithm (5.1) the 'motion' of the phase point in the phase space is given by a sequence $(z_n)_{n=0}^N$ in P. In this case we view the algorithmic solution as being generated by a Δt-advance mapping $\mathbb{F}_{\Delta t} : P \to P$ such that $z_{n+1} = \mathbb{F}_{\Delta t}(z_n)$. For the mid-point algorithm this mapping is defined implicitly by an expression of the form $\mathbb{G}_{\Delta t}(z_n, z_{n+1}) = 0$.

5.2. Properties of the algorithmic flow

The discrete dynamics described by the mid-point algorithm (5.1a) or (5.1b) give rise to an algorithmic flow on P with the following properties.

(1) *Conservation of total angular momentum*. As before, define the angular momentum map $\mathbf{J} : P \to \mathbb{R}^3$ by the expression $\mathbf{J}(z) = q \times p$. Then, $\mathbf{J}$ is preserved along any motion $(z_n)_{n=0}^N$ in the sense that

$$\mathbf{J}(z_{n+1}) = \mathbf{J}(z_n) \,, \quad (n = 0, 1, \ldots, N) \,. \tag{5.2}$$

This result follows directly from the algorithmic equations.

(2) *Symplectic character of the algorithmic flow*. Consider the Δt-advance mapping for the mid-point algorithm defined by the implicit relation (5.1a). Associated with this mapping we have the discrete equation of variations

$$\delta z_{n+1} = \mathbb{A}_{\Delta t}(z_n, z_{n+1}) \, \delta z_n \,, \tag{5.3}$$

where $\mathbb{A}_{\Delta t}(z_n, z_{n+1}) : T_{z_n}P \to T_{z_{n+1}}P$ is the linearized Δt-advance mapping. A straightforward calculation

shows that $\mathbb{A}_{\Delta t}(z_n, z_{n+1})$ satisfies the condition in (3.8) so that the algorithmic Δt-advance mapping defined by the implicit relation (5.1a) is a symplectic map on P with the standard two-form.

5.3. Reduction

Due to the presence of the conserved quantity J the discrete dynamics on P defined by the mid-point algorithm (5.1a) or (5.1b) may be reduced to a phase space $\tilde{P} \subset \mathbb{R}^2$. As before, let $\{e_1, e_2, e_3\}$ be a fixed orthonormal basis in $\mathbb{R}^3$ and consider a motion $(z_n)_{n=0}^N$ in P for which $J(z_0) = \mu \neq 0$. Since J is constant along any motion and by construction $q_n \cdot J = 0$ and $p_n \cdot J = 0$, we conclude that q_n and p_n remain in the plane $\Gamma = \{x \in \mathbb{R}^3 : x \cdot \mu = 0\}$ for $n = 0, 1, \ldots, N$.

Assume for simplicity that μ is parallel to e_3 and introduce plane polar coordinates $(\lambda, \vartheta) \in \mathbb{R}_+ \times S^1$ in Γ. Let $\{e_n, e_n^\perp, e_3\}$ be a moving orthonormal frame defined at each point of the motion by the expressions

$$
\begin{aligned}
e_n &= q_n / |q_n| , \\
e_3 &= \mu / \mu , \\
e_n^\perp &= e_3 \times e_n .
\end{aligned}
\tag{5.4}
$$

At each point of the motion let ϑ_n be defined such that the orientation of e_n with respect to the fixed frame is

$$
e_n = \cos(\vartheta_n) e_1 + \sin(\vartheta_n) e_2 .
\tag{5.5}
$$

From (5.4) we see that $\{e_n, e_n^\perp\}$ span Γ for each n and hence we can express $q_n, q_{n+1} \in \Gamma$ as

$$
\begin{aligned}
q_n &= \lambda_n e_n , \\
q_{n+1} &= \lambda_{n+1} e_{n+1} .
\end{aligned}
\tag{5.6}
$$

To simplify the developments that follow it proves convenient to define a second moving frame $\{\hat{e}, \hat{e}^\perp, e_3\}$ which in each time interval $[t_n, t_{n+1}]$ is given by

$$
\begin{aligned}
\hat{e} &= \frac{e_{n+1} + e_n}{|e_{n+1} + e_n|} , \\
\hat{e}^\perp &= \frac{e_{n+1} - e_n}{|e_{n+1} - e_n|} , \\
e_3 &= \hat{e} \times \hat{e}^\perp = \mu / \mu .
\end{aligned}
\tag{5.7}
$$

Let $\theta = \vartheta_{n+1} - \vartheta_n$ be the angle between the vectors q_{n+1} and q_n, i.e. the swept angle in the interval $[t_n, t_{n+1}]$. Then using the basis in (5.7) we have

$$
\begin{aligned}
e_n &= \cos(\theta/2)\hat{e} - \sin(\theta/2)\hat{e}^\perp , \\
e_{n+1} &= \cos(\theta/2)\hat{e} + \sin(\theta/2)\hat{e}^\perp ,
\end{aligned}
\tag{5.8}
$$

which in view of (5.6) gives

$$
\begin{aligned}
q_n &= \lambda_n \cos(\theta/2)\hat{e} - \lambda_n \sin(\theta/2)\hat{e}^\perp , \\
q_{n+1} &= \lambda_{n+1} \cos(\theta/2)\hat{e} + \lambda_{n+1} \sin(\theta/2)\hat{e}^\perp .
\end{aligned}
\tag{5.9}
$$

We now proceed to express $p_n, p_{n+1} \in \Gamma$ in the moving frame (5.7). As before, at each point in the motion let $\pi_n = p_n \cdot e_n$. By conservation of angular momentum we have $q_n \times p_n = \mu e_3$ and $q_{n+1} \times p_{n+1} = \mu e_3$. Taking the cross product of these expressions with q_n and q_{n+1}, respectively, leads to

$$p_n = \left[\pi_n \cos(\theta/2) + \frac{\mu}{\lambda_n} \sin(\theta/2) \right] \hat{e} - \left[\pi_n \sin(\theta/2) - \frac{\mu}{\lambda_n} \cos(\theta/2) \right] \hat{e}^{\perp} ,$$

$$p_{n+1} = \left[\pi_{n+1} \cos(\theta/2) - \frac{\mu}{\lambda_{n+1}} \sin(\theta/2) \right] \hat{e} + \left[\pi_{n+1} \sin(\theta/2) + \frac{\mu}{\lambda_{n+1}} \cos(\theta/2) \right] \hat{e}^{\perp} .$$

(5.10)

Substituting (5.9) and (5.10) into the mid-point algorithm (5.1b) yields the following component equations for the reduced variables λ, π and θ:

$$\lambda_{n+1} - \lambda_n = \Delta t\, m^{-1} \left[\pi_{n+1/2} + \mu \frac{\lambda_{n+1} - \lambda_n}{2\lambda_n \lambda_{n+1}} \tan(\theta/2) \right] ,$$

$$\pi_{n+1} - \pi_n = -\Delta t\, \sigma \lambda_{n+1/2} + \mu \frac{2\lambda_{n+1/2}}{\lambda_n \lambda_{n+1}} \tan(\theta/2) ,$$

(5.11)

$$2\lambda_{n+1/2} \sin(\theta/2) = \Delta t\, m^{-1} \left[\frac{1}{2} (\pi_{n+1} - \pi_n) \sin(\theta/2) + \mu \frac{\lambda_{n+1/2}}{\lambda_n \lambda_{n+1}} \cos(\theta/2) \right] ,$$

$$2\pi_{n+1/2} \sin(\theta/2) = -\frac{1}{2} \Delta t\, \sigma(\lambda_{n+1} - \lambda_n) \sin(\theta/2) + \mu \frac{\lambda_{n+1} - \lambda_n}{\lambda_n \lambda_{n+1}} \cos(\theta/2) ,$$

(5.12)

where $\sigma = V'(|q_{n+1/2}|)/|q_{n+1/2}|$. Note that there are four equations for three unknown reduced variables λ_{n+1}, π_{n+1} and θ (i.e. ϑ_{n+1}). A simple calculation shows that the dependent equations are those in (5.12). With the proper substitutions these two equations become identical. Solving for the quantity $(\lambda_{n+1} - \lambda_n)$ in $(5.11)_1$ and substituting the result into $(5.12)_2$ yields

$$\tan^2(\theta/2) - \frac{2\lambda_n \lambda_{n+1}}{\Delta t\, m^{-1} \mu} \left(1 + \frac{1}{4} \Delta t^2\, m^{-1} \sigma \right) \tan(\theta/2) + 1 = 0 .$$

(5.13)

Hence, Eqs. (5.12) may be replaced by the single equation (5.13). The reduced algorithmic equations are then

$$\lambda_{n+1} - \lambda_n = \Delta t\, m^{-1} \left[\pi_{n+1/2} + \mu \frac{\lambda_{n+1} - \lambda_n}{2\lambda_n \lambda_{n+1}} \tan(\theta/2) \right] ,$$

$$\pi_{n+1} - \pi_n = -\Delta t\, \sigma \lambda_{n+1/2} + \mu \frac{2\lambda_{n+1/2}}{\lambda_{n+1}} \tan(\theta/2) ,$$

$$\tan^2(\theta/2) - \frac{2\lambda_n \lambda_{n+1}}{\Delta t\, m^{-1} \mu} \left(1 + \frac{1}{4} \Delta t^2\, m^{-1} \sigma \right) \tan(\theta/2) + 1 = 0 .$$

(5.14)

REMARK 5.2. The third equation in (5.14) may be taken to define θ as an implicit function of λ_n and λ_{n+1}. In principle, we could eliminate this equation and end up with a system of the form $\tilde{G}_{\Delta t}(\tilde{z}_n, \tilde{z}_{n+1}) = 0$ where $\tilde{z}_n = (\lambda_n, \pi_n)^{\mathrm{T}} \in \tilde{P}$. That is, we may view (5.14) as defining an implicit map of $\tilde{P} \subset \mathbb{R}^2$ into itself. According to the symplectic reduction theorem, the Δt-advance mapping for the reduced algorithm on $\tilde{P}$ is symplectic given that the algorithm on the canonical phase space P is symplectic.

5.4. Stability of algorithmic relative equilibria

As in the exact case, a fixed point of the reduced algorithmic equations on $\tilde{P}$ corresponds to a steady (discrete) solution of the algorithmic equations on P. This steady solution is then a discrete analog of a relative equilibria. Following the model problem we seek a fixed point $\tilde{z}^* \in \tilde{P}$ of the reduced algorithmic equations (5.14). In the algorithmic case, $\tilde{z}^*$ is a fixed point if there exists a motion $(\tilde{z}_n)_{n=0}^N$ such that $\tilde{z}_n = \tilde{z}^*$ $(n = 0, 1, \ldots, N)$. To this end we have the following

LEMMA 5.1. $\tilde{z}^* = (\lambda^*, 0)^{\mathrm{T}} \in \tilde{P}$ is a fixed point of the reduced algorithmic equations (5.14) if λ^* is a stationary point of an algorithmic amended potential $\hat{V}_{\mu} : \mathbb{R}_+ \to \mathbb{R}$ defined as

$$\hat{V}_\mu(\lambda) = \int_1^\lambda \alpha(s)V'(s/\alpha(s)) \, ds + \mu^2/2m\lambda^2 \,, \tag{5.15}$$

where

$$\alpha(\lambda) = \sqrt{1 + \frac{1}{4}\Omega_F^2(\lambda)} \quad \text{and} \quad \Omega_F(\lambda) = \Delta t \, \mu/m\lambda^2 \,.$$

PROOF. Consider a motion $(\tilde{z}_n)_{n=0}^N$ such that $\tilde{z}_n = (\lambda^*, 0)^T$ for all n. Setting $\lambda_n = \lambda_{n+1} = \lambda^*$ and $\pi_n = \pi_{n+1} = 0$ in $(5.14)_1$ shows that this equation is satisfied identically. From $(5.14)_2$ we get

$$\sigma = \frac{2\mu}{\Delta t(\lambda^*)^2} \tan(\theta/2) \,, \tag{5.16}$$

which upon substitution into $(5.14)_3$ yields

$$\tan(\theta/2) = \frac{\Delta t \, \mu}{2m(\lambda^*)^2} \,. \tag{5.17}$$

In view of (5.17) and (5.16) we see that the reduced algorithmic equations are satisfied by a motion of the form $\tilde{z}_n = (\lambda^*, 0)^T$ $(n = 0, 1, \ldots, N)$ if λ^* satisfies the equation

$$\sigma = \frac{\mu^2}{m(\lambda^*)^4} \,, \tag{5.18}$$

where $\sigma = V'(|q_{n+1/2}|)/|q_{n+1/2}|$. For the motion we are considering we have $q_n = \lambda^* e_n$ and $q_{n+1} = \lambda^* e_{n+1}$, and by definition of θ we have $e_n \cdot e_{n+1} = \cos(\theta)$. Using the definition of $q_{n+1/2}$ and some trigonometric identities we arrive at

$$|q_{n+1/2}| = \lambda^* \cos(\theta/2) \,, \tag{5.19}$$

which in view of (5.17) and some more trigonometric identities yields

$$|q_{n+1/2}| = \frac{\lambda^*}{\left[1 + \frac{1}{4}\left(\frac{\Delta t \, \mu}{m(\lambda^*)^2}\right)^2\right]^{1/2}} \,. \tag{5.20}$$

Substituting (5.20) into (5.18) then shows that λ^* must satisfy

$$\alpha(\lambda^*)V'(\lambda^*/\alpha(\lambda^*)) - \frac{\mu^2}{m(\lambda^*)^3} = 0 \,. \tag{5.21}$$

In view of (5.15) λ^* must be a stationary point of $\hat{V}_\mu$ as claimed. $\quad\square$

Regarding the existence of a zero for the function $\hat{V}'_\mu: \mathbb{R}_+ \to \mathbb{R}$ (and hence the existence of a fixed point for the reduced algorithm) we have the following

LEMMA 5.2. $\hat{V}'_\mu = 0$ *defines* λ^* *as an implicit function of* Δt *in a neighborhood of* $\Delta t = 0$.

PROOF. Consider $\hat{V}'_\mu$ as a function of both λ and Δt. Then the zero level set of $\hat{V}'_\mu$ contains the point $(\lambda^*, \Delta t) = (\lambda_e^*, 0)$ where λ_e^* is the stationary point of the exact amended potential V_μ. Since $\partial_\lambda \hat{V}'_\mu(\lambda_e^*, 0) = V''_\mu(\lambda_e^*) > 0$, the claim follows from the implicit function theorem. $\quad\square$

The above result shows that there is a unique λ^*, and hence fixed point $(\lambda^*, 0)$ of the reduced algorithm, for each $\Delta t > 0$ sufficiently small. The question arises, however, as to what happens for a large range of Δt and how strongly λ^* depends on Δt. To answer these questions we present some numerical results for a specific potential. In particular, we consider the non-linear spring potential to be used in our numerical stability experiments which is of the form
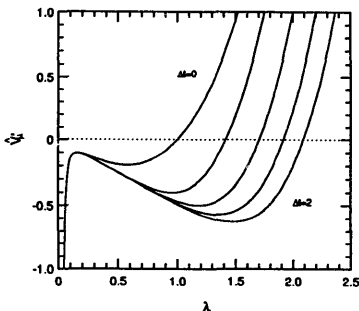
Fig. 1. Plot of $\hat{V}'_\mu$ versus λ (with vertical axis scaled by $1/k$) for time steps in the interval $0 \leq \Delta t \leq 2$. Note that for each time step there exists a unique zero which depends strongly on the time step.

$$V(\lambda) = \frac{1}{2} k(\lambda^2 - \lambda_0^2)^2 . \tag{5.22}$$

Taking for the 'stiff' case $k = 10^6$, $\lambda_0 = 1$, $\mu = 10$, and $m = 1$, in Fig. 1 we plot $\hat{V}'_\mu$ versus λ for a wide range of time steps Δt. Since zeros of $\hat{V}'_\mu$ correspond to stationary points of $\hat{V}_\mu$, the plot shows that there exits a unique stationary point λ^* over a wide range of time steps and that λ^* depends strongly on the time step.

In analogy with the model problem, the algorithmic relative equilibria on P is said to be relatively linearly stable if the fixed point of the reduced algorithmic equations in $\tilde{P}$ is linearly stable. To examine the linear stability of the fixed point we proceed as follows. Invoking the implicit function theorem, the reduced algorithmic equations (5.14) may be written in the form

$$\tilde{G}_{\Delta t}(\tilde{z}_n, \tilde{z}_{n+1}) = 0 , \tag{5.23}$$

where $\tilde{z}_n = (\lambda_n, \pi_n)^T \in \tilde{P} \subset \mathbb{R}^2$. By definition the fixed point $\tilde{z}^* = (\lambda^*, 0)^T$ satisfies $\tilde{G}_{\Delta t}(\tilde{z}^*, \tilde{z}^*) = 0$. Consider an infinitesimal disturbance $\delta\tilde{z}$ on the motion $(\tilde{z}^*)_{n=0}^N$. The infinitesimal disturbance satisfies the discrete equation of variations

$$\delta\tilde{z}_{n+1} = \tilde{A}_{\Delta t}(\tilde{z}^*, \tilde{z}^*) \, \delta\tilde{z}_n , \tag{5.24}$$

where $\tilde{A}_{\Delta t}(z_n, \tilde{z}_{n+1})\colon T_{\tilde{z}_n}\tilde{P} \to T_{\tilde{z}_{n+1}}\tilde{P}$ is the linearized Δt-advance mapping. The fixed point is said to be linearly stable if the linear mapping $\tilde{A}_{\Delta t}(\tilde{z}^*, \tilde{z}^*)$ is stable, i.e. if the eigenvalues $\zeta_{1,2}(\tilde{A}_{\Delta t})$ are simple on the unit circle in the complex plane. If the Δt-advance mapping defined implicitly by relation (5.23) is symplectic on $\tilde{P}$ with the standard two-form, then $\det[\tilde{A}_{\Delta t}(\tilde{z}_n, \tilde{z}_{n+1})] = 1$ along any motion $(\tilde{z}_n)_{n=0}^N$ and the linear stability condition for the fixed point becomes

$$\left| \frac{1}{2} \mathrm{tr}[\tilde{A}_{\Delta t}(\tilde{z}^*, \tilde{z}^*)] \right| < 1 . \tag{5.25}$$

Through a tedious, yet straightforward application of the chain rule we linearize (5.14) (considering θ as an implicit function of λ_n and λ_{n+1}) to obtain the discrete equation of variations. Particularizing this result for the solution $(\tilde{z}^*)_{n=0}^N$ yields (5.24) with a linearized Δt-advance mapping given by

$$\tilde{A}_{\Delta t}(\tilde{z}^*, \tilde{z}^*) = \frac{1}{D}\begin{bmatrix} a & b \\ c & d \end{bmatrix} , \tag{5.26a}$$

where

$$a = 1 - \frac{1}{2}\,\Omega_F^2 - \frac{1}{4}\,\Omega_I^2 - \frac{1}{8}\,\Omega_F\beta(\Omega_I^2 - 3\Omega_F^2 - 8)\,, \qquad b = \Delta t\,m^{-1}\,,$$

$$c = \Delta t^{-1}m\Big(1 - \frac{1}{4}\,\Omega_F^2\Big)\Big[-\Omega_F^2 - \Omega_I^2 - \frac{1}{2}\,\Omega_F\beta(\Omega_I^2 - 3\Omega_{F}^3 - 8)\Big]\,,$$

$$d = 1 - \frac{1}{2}\,\Omega_F^2 - \frac{1}{4}\,\Omega_I^2 - \frac{1}{8}\,\Omega_F\beta(\Omega_I^2 - 3\Omega_F^2 - 8)\,, \qquad\qquad (5.26b)$$

$$D = 1 + \frac{1}{4}\,\Omega_I^2 + \frac{1}{8}\,\Omega_F\beta(\Omega_I^2 - 3\Omega_F^2 - 8)\,,$$

$$\beta = \Big[\Omega_F(1 + \frac{1}{8}\,\Omega_F^2 + \frac{1}{8}\,\Omega_I^2)\Big]\Big/\Big[\frac{1}{8}\,\Omega_F^4 - \frac{1}{16}\,\Omega_F^2\Omega_I^2 - 1\Big]\,,$$

with the sampling frequencies Ω_F and Ω_I defined as

$$\Omega_F = \Delta t\,\mu/m(\lambda^*)^2\,,$$

$$\Omega_I^2 = \Delta t^2\,m^{-1}V''(\lambda^*/\alpha)\,, \qquad \alpha = \sqrt{1 + \frac{1}{4}\Omega_F^2}\,.$$

For this particular solution one may verify that $\det[\bar{\mathbb{A}}_{\Delta t}(\tilde{z}^*, \tilde{z}^*)] = 1$ so that the Δt-advance mapping defined implicitly by (5.23) is a symplectic map on $\tilde{P}$ with the standard two-form along the given motion. (Here, we have used the fact that a mapping of the plane into itself is symplectic with respect to the standard two-form if and only if it is area-preserving.) Regarding the linear stability of the fixed point (and hence the relative linear stability of the relative equilibria) we have the following.

LEMMA 5.3. The relative linear stability limit for the relative equilibria of the mid-point algorithm on P is $\Omega_F \approx 2$.

PROOF. The result follows by direct verification of condition (5.25). From (5.26) we get

$$\frac{1}{2}\,\mathrm{tr}[\bar{\mathbb{A}}_{\Delta t}(\tilde{z}^*, \tilde{z}^*)] = 1 - \frac{2\Omega_F^6 + 2\Omega_F^4\Omega_I^2 + 64\Omega_F^4 + 160\Omega_I^2 + 32\Omega_I^2}{3\Omega_F^6 + 24\Omega_F^4 + 4\Omega_F^2\Omega_I^2 + 64\Omega_F^2 + 16\Omega_I^2 + 64}\,. \qquad (5.27)$$

Considering the 'stiff' case $\Omega_I \gg \Omega_F > 0$ and retaining the highest-order terms in (5.27) gives

$$\frac{1}{2}\,\mathrm{tr}[\bar{\mathbb{A}}_{\Delta t}(\tilde{z}^*, \tilde{z}^*)] \approx 1 - \frac{32 + 2\Omega_F^4}{16 + 4\Omega_F^2}\,, \quad \Omega_I\ \text{large}\,. \qquad (5.28)$$

In view of (5.28) the stability condition (5.25) is satisfied for $0 < \Omega_F < 2$ and violated for $\Omega_F \geqslant 2$. Hence, for the 'stiff' case we have that $\Omega_F \approx 2$ is the relative linear stability limit for the mid-point algorithmic relative equilibria. $\square$

5.5. Algorithmic approximation on reduced phase space

To contrast the results in the preceding sections which were obtained by reducing the mid-point approximation on P, we formulate the mid-point algorithm directly on the reduced space $\tilde{P}$ and address the question of linear stability for fixed points of this formulation. The mid-point approximation to the reduced equations (4.16) is

$$\tilde{z}_{n+1} - \tilde{z}_n = \Delta t\,\tilde{\mathbf{J}}\nabla\tilde{H}(\tilde{z}_{n+1/2})\,, \qquad\qquad (5.29a)$$

where $(\cdot)_{n+1/2} = \frac{1}{2}[(\cdot)_n + (\cdot)_{n+1}]$. In view of $(4.13)_{2,3}$ the explicit form of (5.29a) becomes

$$\lambda_{n+1} - \lambda_n = \Delta t\,m^{-1}\pi_{n+1/2}\,,$$
$$\pi_{n+1} - \pi_n = -\Delta t\,V_\mu'(\lambda_{n+1/2})\,. \qquad\qquad (5.29b)$$

By inspection, a motion of the form $\tilde{z}_n = (\lambda^*, 0)^T$ $(n = 0, 1, \ldots, N)$ satisfies (5.29b) where $\lambda^* = \lambda_c^*$ is a stationary point of the exact amended potential V_μ. Hence, $\tilde{z}^* = (\lambda^*, 0)^T$ is a fixed point for the mid-point algorithm on $\tilde{P}$ and we see that the fixed point of the reduced dynamics is exactly preserved.

To examine the linear stability of the algorithmic fixed point we consider an infinitesimal disturbance $\delta\tilde{z}$ on the motion $(\tilde{z}^*)_{n=0}^N$. The infinitesimal disturbance satisfies the discrete equation of variations

$$\delta\tilde{z}_{n+1} = \tilde{A}_{\Delta t}(\tilde{z}^*, \tilde{z}^*)\,\delta\tilde{z}_n\ , \tag{5.30}$$

where $\tilde{A}_{\Delta t}(\tilde{z}_n, \tilde{z}_{n+1}): T_{\tilde{z}_n}\tilde{P} \to T_{\tilde{z}_{n+1}}\tilde{P}$ is the linearized Δt-advance mapping. Linearizing (5.29b) about the solution $\tilde{z}^*$ yields

$$\tilde{A}_{\Delta t}(\tilde{z}^*, \tilde{z}^*) = \frac{1}{D}\begin{bmatrix} a & b \\ c & d \end{bmatrix}\ , \tag{5.31a}$$

where

$$\begin{aligned}
a &= 1 - \frac{1}{4}\Delta t^2\, m^{-1}V_\mu''(\lambda^*)\ , \\
b &= \Delta t\, m^{-1}\ , \\
c &= -\Delta t\, V_\mu''(\lambda^*)\ , \\
d &= 1 - \frac{1}{4}\Delta t^2\, m^{-1}V_\mu''(\lambda^*)\ , \\
D &= 1 + \frac{1}{4}\Delta t^2\, m^{-1}V_\mu''(\lambda^*)\ .
\end{aligned} \tag{5.31b}$$

As before, the fixed point is said to be linearly stable if the mapping $\tilde{A}_{\Delta t}(\tilde{z}^*, \tilde{z}^*)$ is stable. From (5.31) one can verify that $\det[\tilde{A}_{\Delta t}] = 1$ and $|\frac{1}{2}\,\mathrm{tr}[\tilde{A}_{\Delta t}]| < 1$ so that the mapping $\tilde{A}_{\Delta t}$ and hence the fixed point is unconditionally linearly stable.

6. Conserving approximation

Here, we consider an energy-momentum conserving algorithm and address the question of the relative linear stability for a relative equilibria of this algorithmic approximation. We first outline the construction of a conserving algorithm on P and then reduce the discrete dynamics to $\tilde{P} \subset \mathbb{R}^2$. We then show that the reduced algorithm has a fixed point which is exact and analyze its linear stability. (Note that from general results on discrete Hamiltonian systems with symmetry [17] we know a priori that the reduced scheme will inherit *exactly* the fixed points in the reduced phase space.) For purposes of comparison we formulate a conserving algorithm directly on the reduced space $\tilde{P}$ and perform a similar analysis.

6.1. Algorithm approximation on original phase space

As a point of departure consider the following mid-point approximation to the equations of motion on P:

$$\begin{aligned}
q_{n+1} - q_n &= \Delta t\, m^{-1}p_{n+1/2}\ , \\
p_{n+1} - p_n &= -\Delta t\, \sigma(q_n, q_{n+1})q_{n+1/2}\ ,
\end{aligned} \tag{6.1}$$

where $\sigma: \mathbb{R}^3 \times \mathbb{R} \to \mathbb{R}$ is to be determined and as usual $(\cdot)_{n+1/2} = \frac{1}{2}[(\cdot)_n + (\cdot)_{n+1}]$. From the results for the mid-point rule it follows that the above algorithm preserves the momentum map $J: P \to \mathbb{R}^3$ for any $\sigma(q_n, q_{n+1}) \in \mathbb{R}$. We now proceed to determine σ such that the Hamiltonian (i.e. the total energy) is conserved along any motion $((q_n, p_n))_{n=0}^N$ generated by (6.1). Recall, for the system at hand the Hamiltonian $H: P \to \mathbb{R}$ is separable, of the form $H(z) = K(p) + V(|q|)$ where $K(p) = |p|^2/2m$ is the kinetic energy of the particle. In the interval $[t_n, t_{n+1}]$ the change in kinetic energy is

$$K(p_{n+1}) - K(p_n) = \frac{1}{2} m^{-1}(|p_{n+1}|^2 - |p_n|^2),$$
$$= m^{-1} p_{n+1/2} \cdot (p_{n+1} - p_n).$$
$$\tag{6.2}$$

Substituting the algorithmic equations (6.1) into the above identity yields

$$K(p_{n+1}) - K(p_n) = -\frac{1}{2}(|q_{n+1}|^2 - |q_n|^2)\sigma(q_n, q_{n+1}).$$
$$\tag{6.3}$$

The Hamiltonian is said to be conserved along a motion $(z_n)_{n=0}^N$ if $H(z_{n+1}) = H(z_n)$ for all n. This requires $K(p_{n+1}) - K(p_n) = -[V(|q_{n+1}|) - V(|q_n|)]$ which in view of (6.3) is satisfied by setting

$$\sigma(q_n, q_{n+1}) = \frac{1}{\frac{1}{2}(|q_{n+1}| + |q_n|)} \frac{V(|q_{n+1}|) - V(|q_n|)}{|q_{n+1}| - |q_n|}.$$
$$\tag{6.4}$$

Hence, the discrete dynamics described by (6.1) together with (6.4) give rise to an algorithmic flow on P which preserves exactly the momentum map J and the Hamiltonian H.

REMARKS 6.1.
(1) Note that σ as given in (6.4) is well-defined in the limit as $|q_{n+1}| - |q_n| \to 0$. In practice, when $|q_{n+1}| \approx |q_n|$ we compute σ via an expansion of the form

$$\frac{1}{2}(|q_{n+1}| + |q_n|)\sigma = V'\left(\frac{1}{2}(|q_{n+1}| + |q_n|)\right) + \frac{1}{24}(|q_{n+1}| - |q_n|)^2 V'''\left(\frac{1}{2}(|q_{n+1}| + |q_n|)\right) + \cdots.$$
$$\tag{6.5}$$

(2) The approach outlined above for the construction of an exact energy-momentum preserving algorithm generalizes to more complicated systems such as non-linear elasticity, shells and rods (see [8–10]). For the construction of conserving algorithms for general Hamiltonian systems with more general momentum maps see [17].

6.2. Reduction

Due to the presence of the conserved quantity J the discrete dynamics on P defined by the conserving algorithm (6.1) together with (6.4) may be reduced to a phase space $\tilde{P} \subset \mathbb{R}^2$. Following the same procedure as before yields the reduced equations

$$\lambda_{n+1} - \lambda_n = \Delta t \, m^{-1}\left[\pi_{n+1/2} + \mu \frac{\lambda_{n+1} - \lambda_n}{2\lambda_n \lambda_{n+1}} \tan(\theta/2)\right],$$
$$\pi_{n+1} - \pi_n = -\Delta t \, \sigma \lambda_{n+1/2} + \mu \frac{2\lambda_{n+1/2}}{\lambda_n \lambda_{n+1}} \tan(\theta/2),$$
$$\tan^2(\theta/2) - \frac{2\lambda_n \lambda_{n+1}}{\Delta t \, m^{-1}\mu}\left(1 + \frac{1}{4}\Delta t^2 \, m^{-1}\sigma\right)\tan(\theta/2) + 1 = 0,$$
$$\tag{6.6}$$

where $\sigma = \lambda_{n+1/2}^{-1}[V(\lambda_{n+1}) - V(\lambda_n)]/[\lambda_{n+1} - \lambda_n]$.

6.3. Stability of algorithmic relative equilibria

As before, a fixed point $\tilde{z}^* \in \tilde{P}$ of the reduced algorithmic equations corresponds to a relative equilibria for the algorithm on the original phase space P. Regarding fixed points of the reduced algorithmic equations we have the following:

LEMMA 6.1. $\tilde{z}^* = (\lambda^*, 0)^T \in \tilde{P}$ *is a fixed point of the reduced algorithmic equations (6.6) if* λ^* *is a stationary point of the exact amended potential* $V_\mu : \mathbb{R}_+ \to \mathbb{R}$ *defined as*

$$V_\mu(\lambda) = V(\lambda) + \mu^2/2m\lambda^2 \,. \tag{6.7}$$

PROOF. Consider a motion $(z_n)_{n=0}^N$ such that $\tilde{z}_n = (\lambda^*, 0)^T$ for all n. Setting $\lambda_n = \lambda_{n+1} = \lambda^*$ and $\pi_n = \pi_{n+1} = 0$ in $(6.6)_1$ shows that this equation is satisfied identically. From $(6.6)_2$ we get

$$\sigma = \frac{2\mu}{\Delta t(\lambda^*)^2} \tan(\theta/2) \,, \tag{6.8}$$

which upon substitution into $(6.6)_3$ yields

$$\tan(\theta/2) = \frac{\Delta t\,\mu}{2m(\lambda^*)^2} \,. \tag{6.9}$$

In view of (6.9) and (6.8) we see that the reduced algorithmic equations are satisfied by a motion of the form $\tilde{z}_n = (\lambda^*, 0)^T (n = 0, 1, \ldots, N)$ if λ^* satisfies the equation

$$\sigma = \frac{\mu^2}{m(\lambda^*)^4} \,, \tag{6.10}$$

where we use the expression for σ given in (6.5). For the motion we are considering we have $\lambda_n = \lambda_{n+1} = \lambda^*$ so that (6.10) becomes

$$V'(\lambda^*) - \frac{\mu^2}{m(\lambda^*)^3} = 0 \,. \tag{6.11}$$

Comparing (6.11) to (6.7) shows that λ^* must be a stationary point of V_μ as claimed. $\quad\square$

To examine the linear stability of the fixed point we linearize (6.6) to obtain the discrete equation of variations (5.24). Particularizing this result for the solution $(z^*)_{n=0}^N$ yields a linearized Δt-advance mapping

$$\tilde{\mathbb{A}}_{\Delta t}(\tilde{z}^*, \tilde{z}^*) = \frac{1}{D} \begin{bmatrix} a & b \\ c & d \end{bmatrix} \,, \tag{6.12a}$$

where

$$\begin{aligned}
a &= 1 - \frac{1}{2}\,\Omega_F^2 - \frac{1}{4}\,\Omega_I^2 + \beta\left(1 + \frac{1}{8}\,\Omega_F^2 + \frac{1}{8}\,\Omega_I^2\right), \\
b &= \Delta t\, m^{-1} \,, \\
c &= \Delta t^{-1}\, m\left(1 - \frac{1}{4}\,\Omega_F^2\right)\left[-\Omega_F^2 - \Omega_I^2 + 4\beta\left(1 + \frac{1}{8}\,\Omega_F^2 + \frac{1}{8}\,\Omega_I^2\right)\right], \\
d &= 1 - \frac{1}{2}\,\Omega_F^2 - \frac{1}{4}\,\Omega_I^2 + \beta\left(1 + \frac{1}{8}\,\Omega_F^2 + \frac{1}{8}\,\Omega_I^2\right), \\
D &= 1 + \frac{1}{4}\,\Omega_I^2 - \beta\left(1 + \frac{1}{8}\,\Omega_F^2 + \frac{1}{8}\,\Omega_I^2\right), \\
\beta &= \Omega_F^2\Big/\left[\frac{1}{2}\,\Omega_F^2 - 2\right],
\end{aligned} \tag{6.12b}$$

with the sampling frequencies Ω_F and Ω_I defined as

$$\begin{aligned}
\Omega_F &= \Delta t\,\mu/m(\lambda^*)^2 \,, \\
\Omega_I^2 &= \Delta t^2\, m^{-1} V''(\lambda^*) \,.
\end{aligned}$$

For this solution one may verify that $\det[\tilde{\mathbb{A}}_{\Delta t}(\tilde{z}^*, \tilde{z}^*)] = 1$ so that the stability condition is given by (5.25). Regarding the linear stability of the fixed point we have the following

LEMMA 6.2. *The relative equilibria for the conserving algorithm on P is unconditionally relatively linearly stable.*

PROOF. The result again follows by direct verification of (5.25). From (6.12) we have

$$\frac{1}{2} \text{tr}[\tilde{\mathbb{A}}_{\Delta t}(\tilde{z}^*, \tilde{z}^*)] = 1 - \frac{3\Omega_f^2 + \Omega_I^2}{\frac{1}{8}\Omega_I^4 + \frac{1}{2}\Omega_F^2 + \frac{1}{2}\Omega_I^2 + 2} . \tag{6.13}$$

Making the assumption $\Omega_I \gg \Omega_F > 0$ yields a result independent of Ω_F. To see the effects of Ω_F on (6.13) we proceed as follows. Holding Ω_I fixed, we seek the value of Ω_F, if any, for which (6.13) has a local extrema. Taking the first variation yields $\Omega_F = 2$ as the only stationary point. For this value of Ω_F we get $\frac{1}{2}\text{tr}[\tilde{\mathbb{A}}_{\Delta t}] = -1$ independent of Ω_I. In particular, for any value of Ω_I, we have $|\frac{1}{2}\text{tr}[\tilde{\mathbb{A}}_{\Delta t}]| < 1$ for $0 < \Omega_F < 2$ and $\Omega_F > 2$. Furthermore, one may show using (6.12) that at $\Omega_F = 2$ we have $\tilde{\mathbb{A}}_{\Delta t} = -\text{Iden}$. Hence, tne energy-momentum conserving algorithmic relative equilibria is relatively linearly stable for all $\Omega_F, \Omega_I > 0$. $\square$

REMARKS 6.2.
(1) In accordance with general results for discrete Hamiltonian systems with symmetry we see that the energy-momentum conserving algorithm on the canonical phase space P exactly preserves the fixed point of the reduced dynamics, and hence preserves the relative equilibria of the original system up to group motions.
(2) Since the conserving algorithm inherits the relative Lyapunov stability of the relative equilibria from the underlying system we necessarily have unconditional relative linear stability.

6.4. Algorithmic approximation on reduced phase space

To compare with the results in the preceding sections which were obtained by reducing the algorithmic approximation on *P*, we formulate the algorithm directly on the reduced space $\tilde{P}$ and address the question of linear stability for fixed points of this formulation. Our conserving approximation to the reduced equations (4.16) is

$$\begin{aligned}
\lambda_{n+1} - \lambda_n &= \Delta t \, m^{-1} \pi_{n+1/2} , \\
\pi_{n+1} - \pi_n &= -\Delta t \, \tilde{\sigma}(\lambda_n, \lambda_{n+1}) ,
\end{aligned} \tag{6.14}$$

where $(\cdot)_{n+1/2} = \frac{1}{2}[(\cdot)_n + (\cdot)_{n+1}]$ and σ is of the form

$$\tilde{\sigma}(\lambda_n, \lambda_{n+1}) = \begin{cases} [V_\mu(\lambda_{n+1}) - V_\mu(\lambda_n)] / [\lambda_{n+1} - \lambda_n] . & \lambda_{n+1} \neq \lambda_n ; \\ V'_\mu(\lambda_{n+1/2}) , & \lambda_{n+1} = \lambda_n . \end{cases} \tag{6.15}$$

By inspection, a motion of the form $\tilde{z}_n = (\lambda^*, 0)^T$ ($n = 0, 1, \ldots, N$) satisfies (6.14) where $\lambda^* = \lambda_c^*$ is a stationary point of the exact amended potential V_μ. Hence, $\tilde{z}^* = (\lambda^*, 0)^T$ is a fixed point for the conserving algorithm on $\tilde{P}$ and we see that the fixed point of the reduced dynamics is exactly preserved.

To examine the linear stability of the algorithmic fixed point we consider an infinitesimal disturbance $\delta\tilde{z}$ on the motion $(z^*)_{n=0}^N$. The infinitesimal disturbance satisfies the discrete equation of variations

$$\delta\tilde{z}_{n+1} = \tilde{\mathbb{A}}_{\Delta t}(\tilde{z}^*, \tilde{z}^*) \, \delta\tilde{z}_n , \tag{6.16}$$

where $\tilde{\mathbb{A}}_{\Delta t}(\tilde{z}_n, \tilde{z}_{n+1}): T_{\tilde{z}_n}\tilde{P} \to T_{\tilde{z}_{n+1}}\tilde{P}$ is the linearized Δt-advance mapping. Linearizing (6.14) about the solution $\tilde{z}^*$ yields

$$\tilde{\mathbb{A}}_{\Delta t}(\tilde{z}^*, \tilde{z}^*) = \frac{1}{D} \begin{bmatrix} a & b \\ c & d \end{bmatrix} , \tag{6.17a}$$

where

$$a = 1 - \frac{1}{4} \Delta t^2 \, m^{-1} V''_\mu(\lambda^*) \, ,$$

$$b = \Delta t \, m^{-1} \, ,$$

$$c = -\Delta t \, V''_\mu(\lambda^*) \, ,$$ (6.17b)

$$d = 1 - \frac{1}{4} \Delta t^2 \, m^{-1} V''_\mu(\lambda^*) \, ,$$

$$D = 1 + \frac{1}{4} \Delta t^2 \, m^{-1} V''_\mu(\lambda^*) \, .$$

As before, the fixed point is said to be linearly stable if the mapping $\tilde{\mathbb{A}}_{\Delta_t}(\tilde{z}^*, \tilde{z}^*)$ is stable. From (6.17) one may verify that $\det[\tilde{\mathbb{A}}_{\Delta_t}] = 1$ and $\left| \frac{1}{2} \, \mathrm{tr}[\tilde{\mathbb{A}}_{\Delta_t}] \right| < 1$ so that the mapping $\tilde{\mathbb{A}}_{\Delta_t}$ and hence the fixed point is unconditionally linearly stable.

REMARK 6.3. An important difference between the symplectic mid-point algorithm and the energy-momentum conserving algorithm is that the latter preserves the fixed point of the reduced dynamics regardless of whether it is formulated on the canonical phase space P or the reduced space $\tilde{P}$. This is a reflection of the symmetry properties of the conserving algorithm (see [17]).

7. Numerical example: Verification of stability analysis

In this section we present a numerical example to verify the stability results obtained in the preceding sections. Specifically, we consider the conservative central force problem for a particle of unit mass with a nonlinear spring potential $V : \mathbb{R}_+ \to \mathbb{R}$ of the form

$$V(\lambda) = \frac{1}{2} k(\lambda^2 - 1)^2 \, .$$ (7.1)

For the "stiff" case we take $k = 10^6$ and take as the amplitude of the angular momentum $\mu = 10$.

7.1. Mid-point approximation

To verify the result of the stability analysis of the mid-point algorithm on P we have plotted in Fig. 2 (half) the trace of the amplification matrix (5.27) versus Ω_F. As the plot shows, the stability condition (5.25) for the algorithmic relative equilibria is violated for $\Omega_F > 2$. At the point $\Omega_F \approx 2$ the eigenvalues
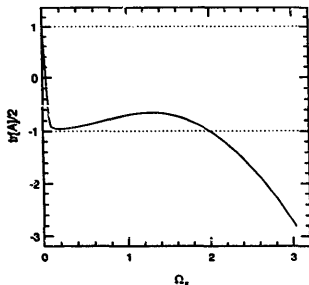

Fig. 2. Trace (up to a factor of one-half) of the linearized Δt-advance mapping for the reduced mid-point algorithm.

of the amplification matrix experience a bifurcation from two complex-conjugate roots with unit modulus into two real roots one of which has modulus greater than unity.

For three values of Δt we integrated the equations of motion on P using (5.1b) and plotted the reduced trajectories in $\tilde{P}$. Figs. 3(a–c) show the fixed point in $\tilde{P}$ and neighboring solutions which were obtained by specifying initial conditions slightly away from the fixed point. Also shown are plots of the total energy versus time for each trajectory. For the plots of the trajectories in $\tilde{P}$ we have scaled the reduced momenta π by a factor of $1/\sqrt{mk}$ to balance the scaling between the π- and λ-axes.

Note the dependence of the location of the fixed point $\tilde{z}^*$ on Δt. In Fig. 3(a) for $\Delta t = 0.01$ we have $\tilde{z}^* \doteq (1.0013, 0)^{\mathrm{T}}$. In Fig. 3(c) for $\Delta t = 0.02$ the fixed point has moved to $\tilde{z}^* \doteq (1.0050, 0)^{\mathrm{T}}$. Also note the
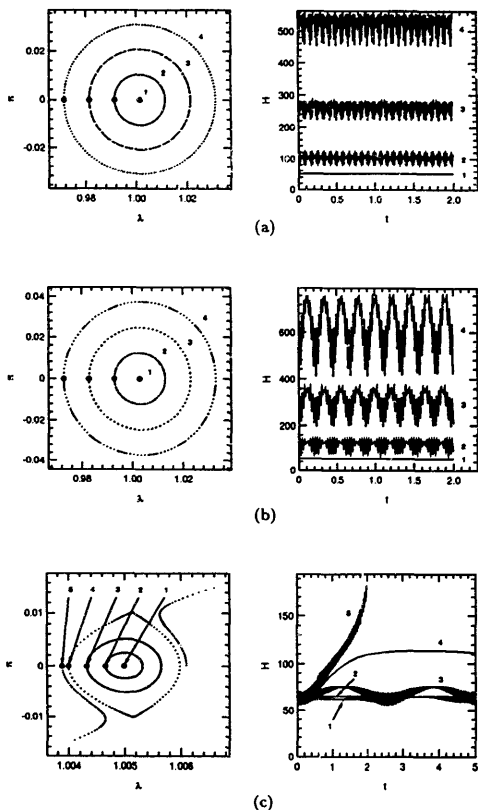
Fig. 3. Reduced phase trajectories and energy plots for the mid-point algorithm on P for (a) $\Delta t = 0.01$ ($\Omega_F \approx 0.1$); (b) $\Delta t = 0.015$ ($\Omega_F \approx 0.15$); (c) $\Delta t = 0.02$ ($\Omega_F \approx 0.2$). ($\bullet$) denotes the initial condition.
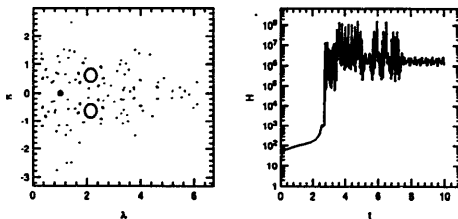
Fig. 4. Spurious solution obtained by continuing computations along curve 5 of the previous figure. (●) denotes the initial condition

size of the stability region in Fig. 3(c). In this figure, curves 1–3 show the fixed point and neighboring solutions which appear qualitatively correct. Slightly further away from the fixed point we have curve 4 in which we begin to see corners in the trajectory. Finally, curve 5 shows a solution which quickly leaves the neighborhood of the fixed point and becomes a spurious solution. Fig. 4 shows the spurious solution which results if we proceed with the computations along curve 5.

Further increases in Δt yield similar behavior, i.e., the fixed point continues to move to the right and the stability region continues to shrink. By $\Delta t = 0.13$ ($\Omega_F \approx 1$) the stability region for the fixed point cannot be resolved due to the precision of the computations. The fixed point itself can be maintained only for a few time steps before roundoff and tolerance errors drive the solution out of the stability region. For some value of Ω_F between 1 and 2 the fixed point vanishes, i.e. it is lost after the first time step.

Fig. 5 shows the result of integrating the reduced equations of motion on $\tilde{P}$ using (5.29b). In this case the solution curves are independent of the time step so that we show only one plot. Here, we note that the fixed point $\tilde{z}^* \doteq (1.0001, 0)^T$ of the reduced dynamics is exactly preserved and that the fixed point does not have a limited stability region.

7.2. Conserving approximation

The results of the stability analysis of the energy-momentum conserving algorithm on P are verified in Fig. 6 where we have plotted (half) the trace of the amplification matrix (6.13) versus Ω_F. As the plot shows, the stability condition (5.25) for the algorithmic relative equilibria is satisfied for all $\Omega_F \geq 0$. The only exception is $\Omega_F = 2$ where we have $|\frac{1}{2} \text{tr}[\overline{\mathbb{A}}_{\Delta t}]| = 1$. This point, however, is still stable as discussed earlier.

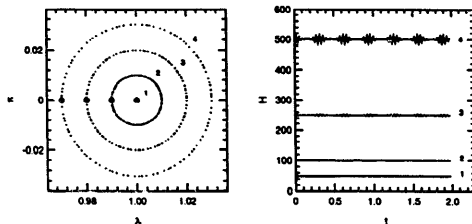Fig. 5. Phase trajectories and energy plots for the mid-point algorithm on $\tilde{P}$. Note that the trajectories are independent of Δt. (●) denotes the initial condition.
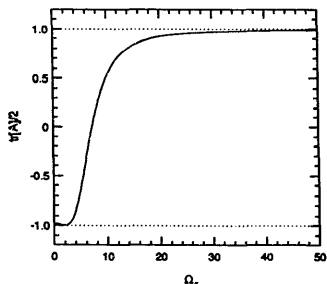
Fig. 6. Trace (up to a factor of one-half) of the linearized Δt-advance mapping for the reduced energy-momentum conserving algorithm.
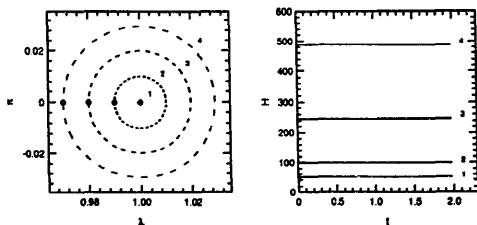

Fig. 7. Reduced phase trajectories and energy plots for the energy-momentum conserving algorithm on P. Note that the trajectories are independent of Δt. (●) denotes the initial condition.

For $\Delta t = 0.02$ we integrated the equations of motion on P using (6.1) together with (6.4) and plotted reduced trajectories in $\tilde{P}$. Fig. 7 shows the fixed point and neighboring solutions as well the energy plots for each trajectory. For the conserving algorithm the location of the fixed point $\tilde{z}^* \doteq (1.0001, 0)^{\mathrm{T}}$ is exact and is independent of Δt, hence we show only one plot. Also, note that this algorithm is not seen to have a limited stability region which decreases with Δt as does the mid-point rule on P.

Fig. 8 shows the result of integrating the reduced equations of motion on $\tilde{P}$ using (6.14). Again, the trajectories are independent of the time step so that we show only one plot. As with the formulation on
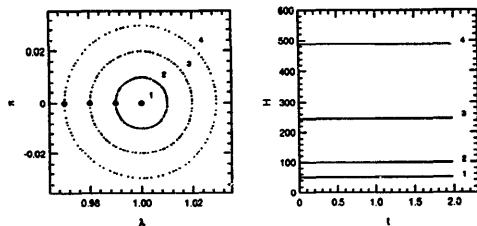

Fig. 8. Phase trajectories and energy plots for the energy-momentum conserving algorithm on $\tilde{P}$. Note that the trajectories are independent of Δt. (●) denotes the initial condition.

P, the fixed point $\bar{z}^* = (1.0001, 0)^T$ of the reduced dynamics is exactly preserved and does not have a limited stability region. Note that the trajectories in this case are identical to those in Fig. 7 which were obtained using the formulation on P.

8. Numerical accuracy comparisons

In this section we perform some numerical experiments to compare the relative accuracy of the symplectic mid-point rule and the energy-momentum conserving scheme. As we saw in the previous section the symplectic mid-point rule can have stability problems for stiff Hamiltonian systems with symmetry. However, for moderately small time steps where the mid-point rule actually performs well, the question arises as to how the relative accuracy of the conserving scheme compares with that of the mid-point rule. Also, it is of interest to know how conserving schemes compare with the mid-point rule for non-stiff problems. In view of these questions we perform our numerical experiments with the central force problem using three different potentials: the classical Kepler potential (non-stiff), a non-linear spring potential with low stiffness, and a non-linear spring potential with high stiffness (as considered in the previous section).

8.1. Classical Kepler potential

In this section we present a numerical accuracy comparison between the symplectic mid-point rule and the conserving scheme (both formulated on the original phase space) for the conservative central force problem with the classical Kepler potential. Specifically, we consider a particle of unit mass under the influence of a central force field with potential $V : \mathbb{R}_+ \to \mathbb{R}$ of the form

$$V(\lambda) = -k/\lambda . \tag{8.1}$$

We take $k = 100$ and use the initial conditions $q_0 = (0.9/\sqrt{2}, 0, 0.9/\sqrt{2})$ and $p_0 = (0, -100/9, 0)$. For the accuracy comparison we will consider the time interval $[0, T]$ with $T = 4.40$ and will consider the relative displacement and momentum errors at time $t = T$. For reference, Fig. 9 shows the trajectory from the above initial condition for the time interval $[0, T]$ computed using the mid-point rule with a relatively small time step (similar results obtained with the conserving scheme).

For the accuracy comparison we computed the solution in the time interval $[0, T]$ for various time steps and plotted the relative displacement error $E_q(T) = |q_{\Delta t}(T) - q_c(T)|/|q_c(T)|$ versus Δt where $q_c(T)$ are the converged displacements at time $t = T$ computed with $\Delta t = 10^{-6}$. Results for the relative momentum error $E_p(T) = |p_{\Delta t}(T) - p_c(T)|/|p_c(T)|$ were computed and plotted in a similar manner. Fig. 10 shows the results for the Kepler potential.

For this example we see that the conserving scheme has substantially smaller displacement and momentum errors as compared to the symplectic mid-point rule.
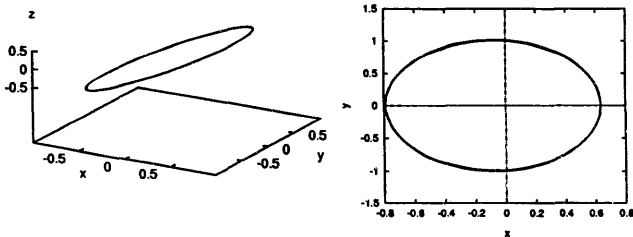

Fig. 9. Numerical trajectory for central force problem with the classical Kepler potential.
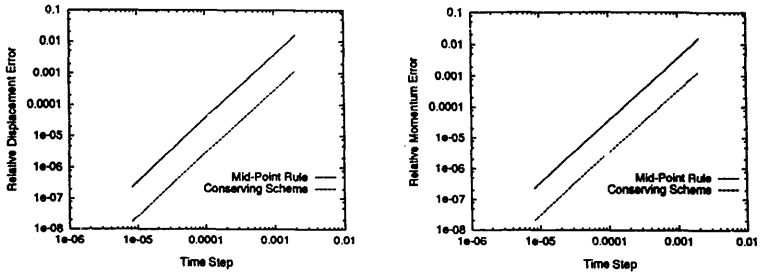
Fig. 10. Relative displacement error $E_q(T)$ and relative momentum error $E_p(T)$ versus time step Δt for the central force problem with the Kepler potential.

8.2. Non-stiff non-linear spring potential

To determine the effect of the force potential on the relative performance of the conserving and mid-point schemes we next consider an example in which the potential is positive-definite (i.e. $V''(\lambda) > 0$) along the motion. This is in contrast to the Kepler potential which is negative-definite along motions. In particular, we consider the central force problem with potential $V : \mathbb{R}_+ \to \mathbb{R}$ of the form

$$V(\lambda) = \tfrac{1}{2} k (\lambda^2 - 1)^2 .\tag{8.2}$$

We take $k = 1000$ and use the initial conditions $q_0 = (0.8/\sqrt{2}, 0, 0.8/\sqrt{2})$ and $p_0 = (0, -100/8, 0)$. For the accuracy comparison we will consider the time interval $[0, T]$ with $T = 0.63$ and will again consider the relative displacement and momentum errors at time $t = T$. For reference, Fig. 11 shows the trajectory from the above initial condition for the time interval $[0, T]$ computed using the mid-point rule with a relatively small time step (similar results obtained with the conserving scheme).

Fig. 12 shows show the results of the accuracy comparison. For this example we see that both schemes exhibit nearly identical displacement errors. With regard to momentum errors, the mid-point rule has a slightly smaller error for a wide range of time steps. However, for small time steps it appears that the opposite may be true. In general, the results show that both schemes have comparable accuracy characteristics for the problem considered. Comparing these results with those for the Kepler potential it is clear that the relative performance of these schemes is problem dependent.
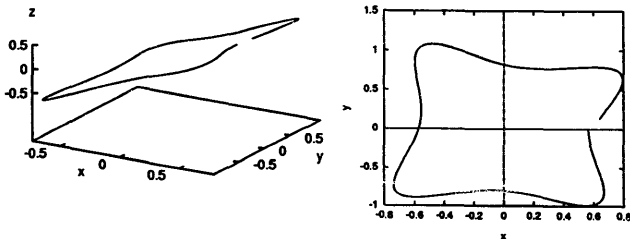

Fig. 11. Numerical trajectory for central force problem with the non-stiff non-linear spring potential.
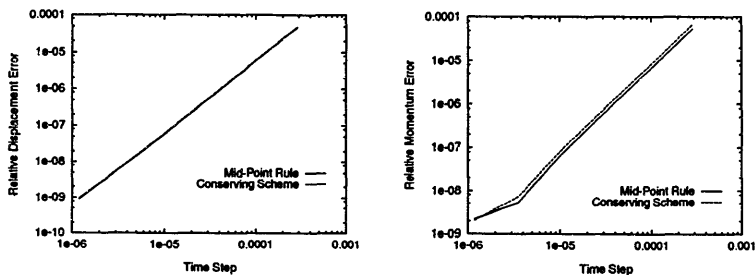
Fig. 12. Relative displacement error $E_q(T)$ and relative momentum error $E_p(T)$ versus time step Δt for the central force problem with the non-stiff nonlinear spring potential.

8.3. Stiff non-linear spring potential

We next consider an example of a stiff system such as that considered in our earlier stability analyses. In particular, we consider a system with a non-linear spring potential V of the same form as before with stiffness constant $k = 10^6$ and use the same initial conditions $q_0 = (0.8/\sqrt{2}, 0, 0.8/\sqrt{2})$ and $p_0 = (0, -100/8, 0)$. For the accuracy comparison we again consider the time interval $[0, T]$ with $T = 0.63$ and consider the relative displacement and momentum errors at time $t = T$. For reference, Fig. 13 shows the trajectory from the above initial condition for the time interval $[0, T]$ computed using the mid-point rule with a relatively small time step (similar results obtained with the conserving scheme). Fig. 14 shows the results of the accuracy comparison.

As we saw earlier the symplectic mid-point rule has stability problems for stiff systems with symmetry. However, the numerical results show that for small time steps the mid-point rule and conserving scheme are nearly indistinguishable from the viewpoint of accuracy. These results suggest that, at the expense of added complexity, the conserving scheme possesses better stability properties than the mid-point rule without a compromise in accuracy, at least for the problems considered herein.
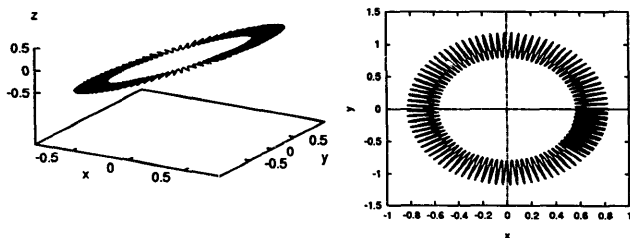

Fig. 13. Numerical trajectory for central force problem with the stiff non-linear spring potential.
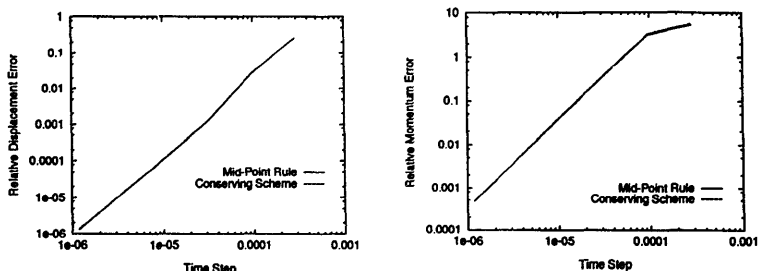
Fig. 14. Relative displacement error $E_x(T)$ and relative momentum error $E_p(T)$ versus time step Δt for the central force problem with the stiff non-linear spring potential.

9. Concluding remarks

Within the context of a simple model problem, we have analyzed the stability of the symplectic mid-point rule and an energy-momentum algorithm. We saw that the mid-point rule formulated on the canonical phase P possessed an algorithmic relative equilibria which depended on the time step and which was only conditionally stable. Also, we have shown by example that the stability region for a 'stable' relative equilibria can decrease dramatically as the time step is increased so that it is practically unstable for time steps substantially below critical. In contrast, the mid-point rule formulated on the reduced space $\tilde{P}$ exactly preserved the relative equilibria of the original system up to group motions. In this setting (i.e. in the absence of group motions) the mid-point rule was shown to possess a fixed point which was unconditionally linearly stable.

As an alternative to the symplectic mid-point rule we introduced an energy-momentum conserving algorithm. We saw that the energy-momentum algorithm formulated on the canonical phase space P had an algorithmic relative equilibria which was independent of the time step, exact up to group motions, and unconditionally linearly stable. Similar results were shown for a conserving algorithm formulated directly on the reduced space.

Our stability analysis confirms a well-observed fact: the symplectic mid-point rule can experience stability problems for stiff systems with symmetry if the time step is not small. Regarding accuracy, our numerical results show that for small time steps the mid-point rule and conserving scheme are nearly indistinguishable. These results suggest that, at the expense of added complexity, the conserving scheme possesses better stability properties than the mid-point rule without a compromise in accuracy, at least for the simple model problems considered in this paper.

References

[1] R. de Vogelaere, Methods of integration which preserve the contact transformation property of Hamiltonian equations, Department of Mathematics, University of Notre Dame, Report 4, 1956.
[2] Feng Kang, Difference schemes for Hamiltonian formalism and symplectic geometry, J. Comput. Math. 4 (1986) 279–289.
[3] Lasagni, Canonical Runge–Kutta methods, ZAMP, 39 (1988) 952–953.
[4] J.M. Sanz-Serna, Runge–Kutta schemes for Hamiltonian systems, BIT 28 (1988) 877–883.

[5] P.J. Chanell and C. Scovel, Symplectic integration of Hamiltonian systems, Nonlinearity 3 (1990) 231–259.

[6] C. Scovel, Symplectic numerical integration of Hamiltonian systems, in: Tudor Ratiu, eds., The Geometry of Hamiltonian Systems, Proc. Workshop held June 5th to 15th, 1989, pp. 463-496, (Springer–Verlag, 1991).

[7] J.M. Sanz-Serna, The numerical integration of Hamiltonian systems, Proc. Conf. on Computational Differential Equations, Imperial College, London, 3–7 July 1989 (1992) in press.

[8] J.C. Simo and N. Tarnow, The discrete energy-momentum method. Conserving algorithms for nonlinear elastodynamics, ZAMP 43 (1992) 757–793.

[9] J.C. Simo and N. Tarnow, A new energy-momentum method for the dynamics of nonlinear shells, Int. J. Numer. Methods Engrg. (1992), in press.

[10] J.C. Simo, N. Tarnow and M. Doblaré, Exact energy-momentum algorithms for the dynamics of nonlinear rods, Int. J. Numer. Methods Engrg. (1993), in press.

[11] J.C. Simo and O. Gonzalez, Assessment of energy-momentum and symplectic schemes for stiff dynamical systems, American Society of Mechanical Engineers, ASME Winter Annual Meeting, New Orleans, Louisiana, 1993.

[12] A. Bayliss and E. Isaacson, How to make your algorithm conservative, Am. Math. Soc. (1975) A594–A595.

[13] R.A. Labudde and D. Greenspan, Energy and momentum conserving methods of arbitrary order for the numerical integration of equations of motion. Part I, Numer. Math. 25 (1976) 323–346.

[14] R.A. Labudde and D. Greenspan, Energy and momentum conserving methods of arbitrary order for the numerical integration of equations of motion. Part II, Numer. Math. 26 (1976) 1–16.

[15] J.C. Simo and K.K. Wong, Unconditionally stable algorithms for rigid body dynamics that exactly preserve energy and angular momentum, Int. J. Numer. Methods Engrg. 31 (1991) 19–52.

[16] M. Austin, P.S. Krishnaprasad and L.C. Chen, Almost Poisson integration of rigid body systems, J. Comput. Phys. 107(1) (1993) 105–117.

[17] O. Gonzalez, Design and analysis of conserving integrators for nonlinear Hamiltonian systems with symmetry, Ph.D. Dissertation, Department of Mechanical Engineering, Division of Applied Mechanics, Stanford University, 1995, to appear.

[18] H. Goldstein, Classical Mechanics, 2nd edition (Addison-Wesley, 1980).

[19] R. Abraham and J.E. Marsden, Foundations of Mechanics, 2nd edition (Addison-Wesley, 1978).

[20] S. Smale, Topology in Mechanics I, Inventiones Math. 10 (1970) 305–331.

[21] S. Smale, Topology in Mechanics II, Inventiones Math. 11 (1970) 45–64.

[22] J.E. Marsden and A. Weinstein, Reduction of symplectic manifolds with symmetry, Rep. Math. Phys. 5 (1974) 121–130.

[23] J.C. Simo, N. Tarnow and K.K. Wong, Exact energy-momentum conserving algorithms and symplectic schemes for nonlinear dynamics, Comput. Methods Appl. Mech. Engrg. 1 (1992) 63-116.